Neurobiology of Disease 139 (2020) 104815

Contents lists available at ScienceDirect

Neurobiology of Disease

journal homepage: www.elsevier.com/locate/ynbdi

Diagnostic and prognostic values of PBMC proteins in amyotrophic lateral sclerosis

Silvia Luotti[a,1], Laura Pasetto[a,1], Luca Porcu[a], Valter Torri[a], Saioa R. Elezgarai[a], Serena Pantalone[a], Melania Filareti[b], Massimo Corbo[b], Christian Lunetta[c], Gabriele Mora[d], Valentina Bonetto[a,*]

[a] Istituto di Ricerche Farmacologiche Mario Negri IRCCS, Milano, Italy
[b] Department of Neurorehabilitation Sciences, Casa Cura Policlinico (CCP), Milano, Italy
[c] NEuroMuscular Omnicentre (NEMO), Serena Onlus Foundation, Milano, Italy
[d] Department of Neurorehabilitation, ICS Maugeri IRCCS, Milano, Italy

A B S T R A C T

Amyotrophic lateral sclerosis (ALS) is a fatal motor neuron disease for which there are no validated biomarkers. Previous exploratory studies have identified a panel of candidate protein biomarkers in peripheral blood mononuclear cells (PBMCs) that include peptidyl-prolyl cis-trans isomerase A (PPIA), heat shock cognate protein 71 kDa (HSC70), heterogeneous nuclear ribonucleoprotein A2/B1 (hnRNPA2B1) and TDP-43. It has also been found that PPIA plays a key role in the assembly and dynamics of ribonucleoprotein (RNP) complexes and interacts with TDP-43. Its absence accelerates disease progression in a SOD1 mouse model of ALS, and low levels of PPIA in PBMCs are associated with early-onset ALS. However, the diagnostic and prognostic values of PPIA and the other candidate protein biomarkers have not been established. We analyzed the PBMC proteins in a well-characterized cohort of ALS patients (n = 93), healthy individuals (n = 104) and disease controls (n = 111). We used a highly controlled sample processing procedure that implies two-step differential detergent fractionation. We found that the levels of the selected PBMC proteins in the soluble and insoluble fraction, combined, have a high discriminatory power for distinguishing ALS from controls, with PPIA, hnRNPA2B1 and TDP-43 being the proteins most closely associated with ALS. We also found a shift toward increased protein partitioning in the insoluble fraction in ALS and this correlated with a worse disease phenotype. In particular, low PPIA soluble levels were associated with six months earlier death. In conclusion, PPIA is a disease modifier with prognostic potential. PBMC proteins indicative of alterations in protein and RNA homeostasis are promising biomarkers of ALS, for diagnosis, prognosis and patient stratification.

1. Introduction

Amyotrophic lateral sclerosis (ALS) is a fatal neurodegenerative disease causing a progressive degeneration of upper and lower motor neurons, resulting in paralysis and death, usually within 20 to 48 months from onset (Chio et al., 2008). Diagnosis is based mainly on clinical evaluation with a history of progression of symptoms and is usually made in about a year (Westeneng et al., 2018). ALS is clinically, genetically and neuropathologically highly heterogeneous, which makes the identification of biomarkers and development of effective therapies challenging (Beghi et al., 2011). There are still no validated biomarkers for early diagnosis, prognosis, to monitor the progression of the disease, stratify patients and assess the efficacy of new treatments (Chipika et al., 2019).

Several studies have shown that neurofilaments (NFs) are elevated in cerebrospinal fluid (CSF) and blood of patients with ALS, even at a presymptomatic stage (Benatar et al., 2018; De Schaepdryver et al., 2019), and at the moment these are the most promising molecular biomarkers with diagnostic value (Verde et al., 2019a; Feneberg et al., 2018; Steinacker et al., 2016). There is also growing evidence of the potential utility of NFs in predicting prognosis and monitoring treatment efficacy (Poesen and Van Damme, 2018). However, NFs reflect neuroaxonal injury and are high not only in ALS, but in other neurodegenerative diseases too (Khalil et al., 2018). Their diagnostic and prognostic value is higher in CSF, which is a more invasive source of biomarkers than in blood (Verde et al., 2019b). Results have been promising for the NF light chain in serum (Verde et al., 2019a; Feneberg et al., 2018), but only fourth-generation single-molecule array technology can detect the whole range of concentrations in blood (Disanto et al., 2017).

TAR DNA-binding protein 43 (TDP-43) is a nuclear RNA binding protein that regulates several steps of RNA metabolism (Lagier-

* Corresponding author at: Department of Biochemistry and Molecular Pharmacology, Istituto di Ricerche Farmacologiche Mario Negri IRCCS, Via Mario Negri 2, 20156 Milano, Italy.
E-mail address: valentina.bonetto@marionegri.it (V. Bonetto).
[1] These authors contributed equally to this work.

https://doi.org/10.1016/j.nbd.2020.104815
Received 9 December 2019; Received in revised form 14 February 2020; Accepted 18 February 2020
Available online 20 February 2020

Tourenne et al., 2010). Upon stress, TDP-43 is recruited into stress granules and this may lead to its persistent accumulation in the cytoplasm (Fang et al., 2019; Parker et al., 2012). With 2–3% of ALS patients carrying mutations in TDP-43 and ~97% of all ALS cases presenting TDP-43 pathology, TDP-43 is likely to be involved in a key pathogenic mechanism common to all forms of the disease. It is therefore an interesting biomarker to detect in biological fluids. However, none of the studies so far in CSF or blood have reported encouraging results for its use in diagnosis or prognosis and there are no surrogate biomarkers reflecting TDP-43 pathology (Verde et al., 2019b).

Motor neuron degeneration is a non-cell autonomous process (Ilieva et al., 2009). A neuroinflammatory reaction consisting of a complex interplay between activated glial cells and immune cells seems to have an impact on the onset and progression of the disease (Beers and Appel, 2019). It would be important to identify biomarkers for monitoring the efficacy of new drugs targeting such mechanisms. Peripheral blood mononuclear cells (PBMCs), which are mainly lymphocytes and monocytes, are an accessible and feasible source of human cells for this purpose. They display pathological features mirroring those occurring in the central nervous system, including TDP-43 cytoplasmic mislocalization (Nardo et al., 2011; Filareti et al., 2017; De Marco et al., 2011; Mougeot et al., 2011; De Marco et al., 2017). In exploratory studies in PBMCs of ALS patients, we identified protein profile changes in comparison with controls indicative of alterations in protein and RNA homeostasis (Nardo et al., 2011; Filareti et al., 2017). In particular, PBMC levels of peptidyl-prolyl cis-trans isomerase A (PPIA), also known as cyclophilin A, heat shock cognate protein 71 kDa (HSC70), heterogeneous nuclear ribonucleoprotein A2/B1 (hnRNPA2B1) and TDP-43 distinguished ALS patients from healthy controls and, in the case of PPIA, also from those with other neurological diseases (Nardo et al., 2011).

PPIA is a multifunctional protein: a foldase (Fischer et al., 1989), a molecular chaperone (Freskgård et al., 1992), and an interactor of RNA-binding proteins (Pan et al., 2008; Lauranzano et al., 2015). PPIA binds TDP-43 in the low-complexity domain and regulates its function (Lauranzano et al., 2015). It affects TDP-43-dependent expression of genes involved in the clearance of protein aggregates, and plays a role in the assembly and dynamics of ribonucleoprotein (RNP) complexes (Pan et al., 2008; Lauranzano et al., 2015). Patients with early disease onset have low PPIA levels in PBMCs (Filareti et al., 2017). Accordingly, the absence of PPIA in the SOD1 mouse model of ALS exacerbates aggregation and accelerates disease progression, indicating that PPIA is a disease modifier (Lauranzano et al., 2015). HSC70, a constitutively expressed member of the heat shock protein 70 family, is a molecular chaperone involved in protein folding and degradation in normal and stress conditions (Liu et al., 2012). It was found sequestered in protein aggregates in the spinal cord of the SOD1 mouse model and sporadic ALS patients (Basso et al., 2009). HnRNPA2B1 shares many characteristics with TDP-43. It is involved in all aspects of RNA processing, contains two RNA recognition motifs, has a glycine-rich low-complexity domain that makes it prone to aggregation, and interacts with PPIA within RNP complexes (Lauranzano et al., 2015). Mutations within the hnRNPA2B1 gene have been associated with multisystem proteinopathy and ALS, although they are exceedingly rare (Kim et al., 2013; Calini et al., 2013).

In this study, we investigated further in a large, well-characterized cohort of ALS patients, whether changes in PBMC protein levels could be of use in diagnosis, prognosis and patient stratification. We established a highly controlled procedure for sample collection, protein extraction and immunoassays that can be easily implemented in any laboratory.

2. Materials and methods

2.1. ALS patients and control subjects

The study was approved by the Ethics Committees of the clinical centers involved: ICS Maugeri IRCCS, Milano, NEuroMuscular Omnicentre (NEMO), Milano, Casa Cura Policlinico, Milano, and written informed consent was obtained from all subjects. The diagnosis of ALS was based on a detailed medical history and physical examination, and supported by electrophysiological evaluation. Inclusion criteria for ALS patients were: i) 18–85 years of age; ii) diagnosis of definite, probable or laboratory-supported probable ALS, according to revised El Escorial criteria (Brooks et al., 2000); iii) signs of disease progression in the last three months; iv) treatment with riluzole (100 mg a day) for at least 30 days. Exclusion criteria were: i) familial ALS; ii) diabetes or severe inflammatory conditions; iii) active malignancy; iv) pregnancy or breast-feeding. For some analyses, ALS patients were stratified according to the rate of disease progression expressed as ΔALSFRS-R (48-ALSFRS-R)/disease duration in months), as slow ALS with ΔALSFRS-R $\leq$ 0.5, moderate ALS with ΔALSFRS-R $>$ 0.5 and $<$ 1, and fast ALS with ΔALSFRS-R $\geq$ 1, as described by (Kimura et al., 2006). Symptom duration was defined as the time (in months) from symptom onset to blood withdrawal. Survival was considered as the time (in months) from blood withdrawal to death or tracheostomy. The control subjects were: healthy individuals (Healthy) (n = 104) and subjects with other neurological/neuromuscular diseases (n = 111). Controls patients were grouped in patients with diseases affecting the central nervous system (CNS controls) (n = 63) and patients with diseases affecting the peripheral nervous system or muscles (Periphery controls) (n = 48). CNS controls were: ischemic stroke (n = 15), hemorrhagic stroke (n = 12), unspecified stroke (n = 12), Parkinson's disease (n = 15), multiple sclerosis (n = 4), progressive supranuclear palsy (n = 2), multisystem atrophy (n = 2), fragile X-associated tremor/ataxia syndrome (n = 1); and patients with diseases affecting the peripheral nervous system (Periphery controls) (n = 48): myotonic dystrophy type 1 (n = 15), limb-girdle muscular dystrophy (n = 8), facioscapulohumeral muscular dystrophy (n = 6), Becker muscular dystrophy (n = 3), myotonic dystrophy type 2 (n = 1), Duchenne muscular dystrophy (n = 1), Emery-Dreifuss muscular dystrophy (n = 1), peripheral neuropathy (n = 5), myasthenia gravis (n = 3), Charcot–Marie–Tooth disease (n = 2), inclusion body myositis (n = 2), mitochondrial myopathy (n = 1). The main characteristics of the subjects involved in the study are summarized in Table 1.

2.2. Blood collection and PBMC isolation

Blood was drawn by standard venipuncture at the clinical centers in 6-mL Vacutainer® Plus Plastic K2EDTA Tubes (Becton, Dickinson and Company), kept at 4 °C and shipped as soon as possible to the Istituto di Ricerche Farmacologiche Mario Negri IRCCS, where PBMC isolation was started not more than 4h after blood collection, as follows:

1. Dilute blood (1:1) with room-temperature RPMI 1640 medium (Lonza).
2. Fill 50 mL-Falcon tubes with room-temperature Ficoll-Paque Plus (GE Healthcare) (7 mL per 10 mL diluted blood).
3. Underlay carefully diluted blood into each tube, avoid mixing the two layers.
4. Centrifuge at 800 $\times g$ for 30 min (brake off) at 18–20 °C.
5. Pipette off most of the plasma, and discard.
6. Carefully aspirate the buffy coat and transfer it into 15 mL-Falcon tubes, avoiding aspirating the Ficoll-Paque layer (granulocyte contamination).
7. Cell washings (four times):

- add three volumes of RPMI and centrifuge at 400 $\times g$ for 15 min at

Table 1
Characteristics of ALS patients and control subjects.

Characteristics	ALS	Healthy	CNS[1]	Periphery[2]
N	93	104	63	48
Age at sampling, years median (range)	65 (38-87)	62 (37-87)	72 (43-90)	52 (32-87)
Sex (male/female)	50/43	48/56	34/29	23/25
Site of disease onset (bulbar/spinal/unknown)	25/65/3	-	-	-
ALSFRS-R at sampling, median (range)	25 (8-46)	-	-	-
ΔALSFRS-R[3], median (range)	0.8 (0.2-9.0)	-	-	-
Slow-ALS (ΔALSFRS-R ≤ 0.5) (n)	18	-	-	-
Moderate-ALS (ΔALSFRS-R > 0.5, < 1) (n)	35	-	-	-
Fast-ALS (ΔALSFRS-R ≥ 1) (n)	40	-	-	-
Symptom duration[4], median (range)	22 (3-146)	-	-	-
Survival[5], median (95% CI)	14.5 (9.5-17.4)			

[1] CNS: Control subjects with diseases affecting the central nervous system (CNS controls).
[2] Periphery: control subjects with diseases affecting the peripheral nervous system or muscles (Periphery controls).
[3] ΔALSFRS-R: 48–ALSFRS-R score at sampling/time from symptom onset to sampling.
[4] Symptom duration: time from symptom onset to sampling (months).
[5] Survival: time from sampling to death or tracheostomy (months); follow-up data were available for 66 ALS patients.

18–20 °C, to remove plasma and platelets
- pipette off supernatant, suspend cells in RPMI, and centrifuge at 200 ×*g* for 10 min at 18–20 °C, to remove platelets
- pipette off supernatant, suspend cells in RPMI, centrifuge at 300 ×*g* for 10 min at 18–20 °C
- pipette off supernatant, suspend cells in RPMI, divide into aliquots in 1.5-mL tubes and centrifuge at 300 ×*g* for 10 min at 18–20 °C

8. Pipette off supernatant and store PBMC pellet vials at -70 °C until protein extraction.

2.3. Protein extraction

PBMC pellets (n = 308) were processed in the same day (step 1) by four operators each processing six samples at the time (Fig. 1). PBMC pellets were placed on ice, suspended with pre-warmed at 95 °C buffer 1 (20 mM Tris-HCl pH 7.5, 0.1% NP40, 0.1% SDS, cOmplete™ Protease Inhibitor Cocktail Tablets in EASYpacks, Roche, 1 tablet /10 ml buffer), and vortexed for 30 s. Samples were kept at 95 °C and shaken at 800 rpm for 5 min in a Thermomixer Comfort (Eppendorf), then centrifuged at 16.000 ×*g* for 10 min at 4 °C. The supernatants were collected and kept on ice, while the pellets were stored at -70 °C until further processing (step 2). Protein in supernatants were quantified by Quick Start™ Bradford Protein Assay (Bio-Rad) using a Zephyr® liquid handler workstation (Perkin Elmer). Supernatants were split into aliquots ready for slot blot (6 μg of total protein lysate diluted with 200 μL Tris-buffered saline, pH 7.5) and stored at -70 °C until protein analysis (PBMC-soluble). In step 2, insoluble pellets were processed the same day by four operators each processing six samples at a time. Samples were placed on ice, suspended with buffer 2 (1% SDS at 95 °C) and

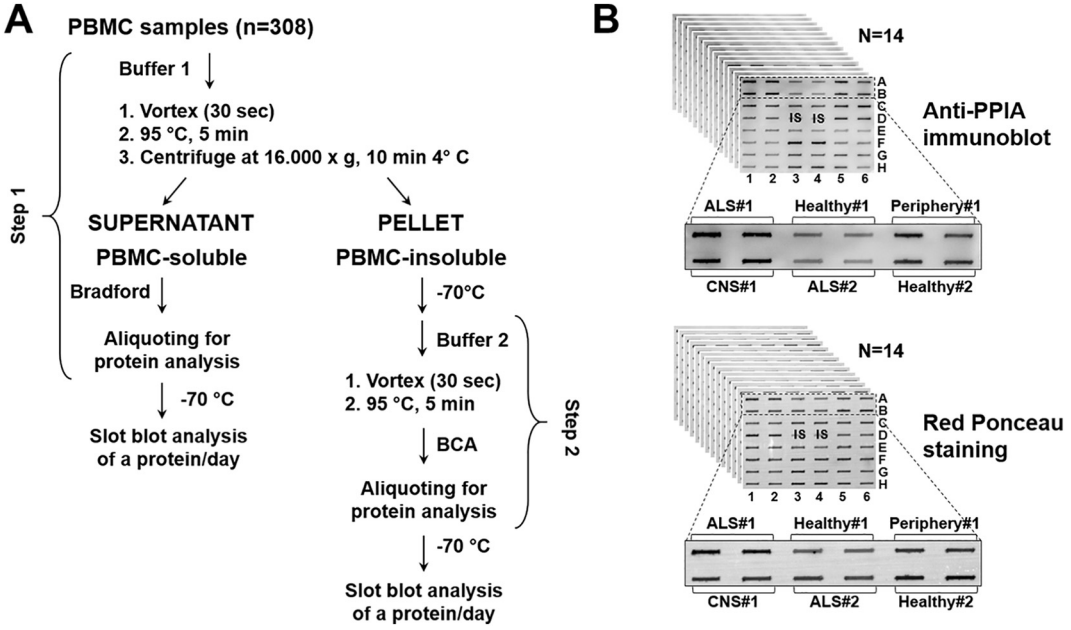

Fig. 1. (A) Schematic workflow for the sequential protein extraction procedure of PBMC samples. To limit intra- and inter-assay variability, all samples (n = 308), from ALS patients and controls, were processed the same day. In step 1 PBMC-soluble was purified from PBMC-insoluble, which was stored at -70 °C and further processed in step 2. (B) PBMC-soluble and PBMC-insoluble were then analyzed for the levels of PPIA, HSC70, TDP-43, hnRNPA2B1 and SOD1 candidate biomarkers by slot blot, performing for each protein, multiple 48-well slots (n = 14) with all PBMC samples and internal standard (IS) in duplicate the same day. A representative set of slot blots for PPIA is shown, with the anti-PPIA immunoblots and the Red Ponceau-stained blots respectively in the upper and lower parts of the panel. ALS samples and controls were alternately loaded on the membrane with the internal standard (IS) always in positions D3 and D4. Immunoreactivity was normalized to Red Ponceau staining and to the immunosignal of the IS of each 48-well slot.

vortexed for 30 s. Samples were kept at 95 °C and shaken at 800 rpm for 5 min in the Thermomixer. Protein quantification was done with a Pierce™ BCA Protein Assay Kit (Thermo Fisher Scientific) on the Zephyr liquid handler. Samples were split into aliquots ready for slot blot (6 μg of total protein lysate diluted with 200 μL Tris-buffered saline, pH 7.5), and stored at -70 °C until protein analysis (PBMC-insoluble). An index of protein insolubility was calculated as the ratio of total protein μg in the PBMC-insoluble to total protein μg in the PBMC-soluble for each sample.

2.4. Western blot analysis

Western blot analyses with pools (n = 10) of PBMC samples from ALS and control subjects were done to verify antibody specificity before slot blot analysis, and to investigate protein partitioning (Supplementary Figs. 1–3). The main characteristics of the subjects analyzed are summarized in Supplementary Table 2. Proteins quantified by the BCA protein assay (Pierce) (25 μg) were suspended in Laemmli sample buffer, separated by electrophoresis on 12% polyacrylamide gels and transferred onto PVDF membranes (Millipore), as previously described (Pasanen et al., 2014). Blots were probed with the following primary antibodies: rabbit polyclonal anti-PPIA (Millipore, RRID: AB_2252847, 1:2500 dilution), rabbit polyclonal anti-TDP-43 (Proteintech, RRID: AB_2200505, 1:2500 dilution), mouse monoclonal anti-hnRNPA2B1 (Abnova, RRID: AB_2117203, 1:2500 dilution), mouse monoclonal anti-HSC70 (Santa Cruz, RRID: AB_627761, 1:1000 dilution), rabbit polyclonal anti-SOD1 (StressMarq, RRID: AB_2704232, 1:1000 dilution), rabbit polyclonal anti-TIA1 (Proteintech, RRID:AB_2201427, 1:1000), rabbit polyclonal anti-G3BP1 (Proteintech, RRID: AB_2232034, 1:2500 dilution), rabbit polyclonal anti-ubiquitin (Dako, RRID:AB_2315524, 1:800), mouse monoclonal anti-SQSTM1/p62 (Abcam, RRID: AB_945626, 1:500). Next, blots were incubated with peroxidase-conjugated secondary antibodies (Santa Cruz Biotechnology) and developed with Luminata™ Forte Western Chemiluminescent HRP Substrate (Millipore) on the ChemiDoc™ Imaging System (Bio-Rad). Densitometry was done with Image Lab software v 6.0 (Bio-Rad). Immunoreactivity was normalized to the Red Ponceau staining (Fluka). Partitioning in PBMC-soluble and PBMC-insoluble was expressed as percentages of the total protein level.

2.5. Slot blot analysis

Slot blot on a 48-well was used for the analysis of PPIA, TDP-43, hnRNPA2B1, HSC70 and SOD1. The primary antibodies and dilutions were the same as for Western blot analysis. To minimize inter-assay variability, slot blot analysis with all samples (n = 308) was done for each protein on multiple 48-well slots the same day (Fig. 1). Aliquots of protein lysates were thawed on ice, vortexed for 30 s, and directly loaded in duplicate onto Immobilon-P PVDF membranes (Merck), by vacuum filtration using a Bio-Dot SF microfiltration apparatus (Bio-Rad). The amount of protein lysate loaded on each well (3 μg) and the dilution of the specific primary antibody used generated results in the linear range for the protein assays. The linearity of the assays for the PBMC proteins was confirmed by serial dilution experiments. An internal standard (IS), a pool of all samples in the analysis, was deposited in duplicate on each 48-well slot blot (Fig. 1B). ALS samples and controls were alternately loaded on the membrane. Membranes were blocked with 3% (w/v) BSA (Sigma) and 0.1% (v/v) Tween 20 in Tris-buffered saline, pH 7.5, incubated with primary antibodies, then with peroxidase-conjugated secondary antibodies (Santa Cruz Biotechnology). Blots were developed with Luminata™ Forte Western Chemiluminescent HRP Substrate (Millipore) on the ChemiDoc™ Imaging System (Bio-Rad). Densitometry was done with Progenesis PG240 v2006 software (Nonlinear Dynamics). Immunoreactivity was normalized to the Red Ponceau staining (Fluka) and to the immunosignal of the internal standard (IS) of each membrane. Data are expressed as arbitrary units (A.U.).

2.6. Statistical analysis

The multinomial logistic regression model was used to detect and calculate differences in the distribution of the PBMC biochemical parameters. Post hoc tests based on Bonferroni correction were used to identify the primary pairwise comparison explaining the differences. To assess the diagnostic performance of the biomarkers alone or combined, a receiver operating characteristics curve (ROC curve) was constructed, and the area under the curve (AUC), with 95% confidence interval (95% CI), was calculated using the logistic regression model. To estimate the AUC of the combined biomarkers we applied the following statistical procedure: (i) a single conditional imputation of missing values for all candidate predictors was done with the R *transcan* function with the following option: imputed = T, transformed = T, impact = "score"; (ii) a full multivariable model with a linear combination of predictors on the original scale was fitted; (iii) a fast-backward step-down procedure with total residual Akaike information criterion as the stopping rule was investigated by the R *fastbw* function, to address overfitting of the multivariable model and identify the predictors that explain the bulk of the ALS condition. Discriminant function analysis method was used to find the optimal cut-off from the ROC curve from which sensitivity, specificity and correct classification were derived. Pearson's correlation coefficient (r) was calculated to measure the linear strength of the association between biomarkers and the clinical characteristics of ALS patients (ALSFRS-R, ΔALSFRS-R, and symptom duration at sampling). Disease duration was defined as the time between sampling and death or tracheostomy, whichever occured first. Biomarkers were evaluated as predictors of disease duration using the Cox regression model. The Kaplan-Meier method was used to estimate survival distributions. The reverse Kaplan-Meier method was used to estimate the length of follow-up. We stratified patients for high or low levels of biomarkers, using the median as a cut-off, because of the limited number of patients with follow-up data. Non-parametric statistics (median, interquartile range and range) were used to describe biomarker distributions. Statistical analyses were done using Prism 7 (GraphPad, version 7.02) and SAS software, version 9.4. Regression modelling strategies were done with R statistical software, version 3.5.0.

3. Results

3.1. High-throughput analysis of PBMC proteins from ALS patients and controls

The study comprised 308 PBMC samples from ALS patients (n = 93), healthy subjects (n = 104), and patients with other diseases (n = 111), grouped as those with diseases affecting the central nervous system (CNS controls) and those with diseases affecting the peripheral nervous system or muscles (Periphery controls). The main demographic and clinical characteristics of the subjects involved in the study are set out in Table 1. Controlled procedures were followed for each step of the study, from blood collection and PBMC isolation to protein extraction and analysis, as described in the Methods section. Proteins were extracted from PBMC pellets the same day for all samples, to limit inter-assay variability, using a two-step differential detergent fractionation method (Fig. 1A). PBMC lysates with buffer 1 mainly comprised highly soluble proteins so we defined it as the soluble fraction (PBMC-soluble). From step 1 extraction we obtained a pellet that was further extracted with 1%-SDS solution (step 2), isolating a protein fraction defined as PBMC-insoluble. Finally, PPIA, HSC70, hnRNPA2B1 and TDP-43 were analyzed by slot blot in PBMC-soluble and PBMC-insoluble, examining multiple 48-well slots for each protein with all PBMC samples the same day (Fig. 1B).

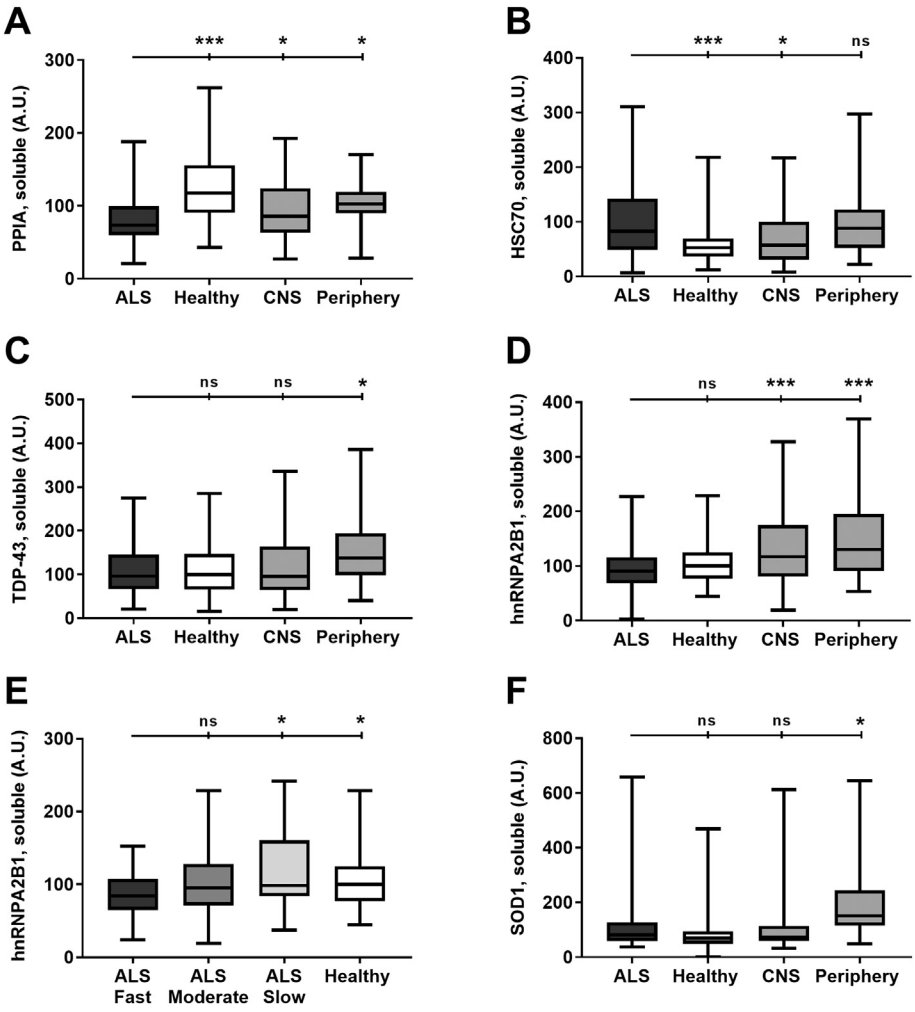

Fig. 2. Analysis of candidate biomarkers in the soluble fraction of PBMC samples (PBMC-soluble) isolated from ALS patients and controls. (A–F) PPIA, HSC70, TDP-43, hnRNPA2B1 and SOD1 were analyzed by slot blot in PBMC-soluble from ALS patients (n = 93), healthy subjects (n = 104), CNS controls (CNS) (n = 63) or Periphery controls (Periphery) (n = 48). (E) The levels of hnRNPA2B1 in ALS patients, stratified by rate of disease progression in fast, moderate and slow were compared with those in Healthy controls. Box plots indicate immunoreactivity normalized to total protein loading and to the internal standard, in arbitrary units (A.U.). In all cases the proteins were differently distributed in the four groups (Table 2). Protein levels different from ALS (A-D, F) or fast ALS (E), with $p < 0.05$ (*), $p < 0.001$ (***); ns, not significantly different from ALS (A-D, F) or fast ALS (E).

3.2. Soluble PBMC proteins

The levels of PPIA, HSC70, TDP-43 and hnRNPA2B1 were analyzed in PBMC-soluble isolated from ALS patients and controls (Healthy, CNS and Periphery controls) (Fig. 2). In all cases the proteins were distributed differently in the four groups in univariate analysis and in multivariate analysis, adjusting for age and sex (Table 2, Supplementary Table 1). Soluble PPIA and HSC70 in ALS patients were different respect to Healthy controls, while soluble hnRNPA2B1 and TDP-43 were not (Fig. 2A–D); PPIA and HSC70 were respectively lower and higher in ALS than in Healthy controls. HSC70 in ALS was also higher than in CNS controls. Soluble hnRNPA2B1and PPIA were lower than in CNS and Periphery controls, while TDP-43 was lower only than Periphery controls. When we stratified ALS patients on the basis of the rate of disease progression (ΔALSFRS-R), as fast, moderate or slow ALS, we observed a progressively lower level of soluble hnRNPA2B1 as the rate of disease progression rose (Fig. 2E). No difference was found for PPIA, HSC70, TDP-43 in ALS patients with different disease progression rates (data not shown).

3.3. Insoluble PBMC proteins

From step 1 extraction a pellet was obtained containing hydrophobic membrane proteins, multiprotein complexes and in general supramolecular assemblies with limited solubility. We defined the ratio of the amount of total protein in PBMC-insoluble to that in PBMC-soluble as the insolubility index, and we calculated this index for each PBMC sample (Fig. 3, Table 2, Supplementary Table 1). It was higher in the pathological controls than in Healthy controls. In particular, it was highest in ALS patients and significantly different from Healthy and Periphery controls, but not from CNS controls. We further characterized the PBMC-insoluble by measuring markers of ALS pathology in a pool of PBMC samples from ALS patients and Healthy, CNS and Periphery controls (see Supplementary Table 2 for clinical characteristics). The insoluble fraction in all pathological conditions was enriched in TDP-43 and its 35 kDa TDP-43 fragment, while the 25 kDa TDP-43 fragment was specifically enriched in ALS samples (Supplementary Fig. 2C–F). PBMC-insoluble was also enriched in TIA1 and G3BP1, markers of stress granules, SQSTM1/p62, a marker of protein inclusions, but not in ubiquitin (Supplementary Fig. 3A–D). There was a shift toward increased partitioning in the PBMC-insoluble for hnRNPA2B1, in all pathological conditions, while for PPIA and SOD1, this was seen only in ALS patients (Supplementary Fig. 2A,G,H). Cereda et al. (Cereda et al., 2013) reported higher levels of insoluble SOD1 in PBMCs of sporadic ALS patients compared to healthy individuals. We measured SOD1 in our patients and controls, in the PBMC-soluble and insoluble (Figs. 2F and 4F). Soluble SOD1 in ALS patients was not different from Healthy and CNS controls, but was high in Periphery controls compared to all the other experimental groups (Fig. 2F). Insoluble SOD1 was higher in ALS patients than in Healthy but lower than in Periphery and CNS controls (Fig. 4F). Finally, a high molecular weight isoform of PPIA was abundantly present only in ALS patients (Supplementary Fig. 1A), a finding that deserves further investigations.

We next measured PPIA, HSC70, TDP-43 and hnRNPA2B1 in PBMC-insoluble by the slot blot approach with the single samples (Fig. 4). In all cases the proteins in the PBMC-insoluble were distributed differently

Table 2
Univariate analysis of PBMC biochemical parameters in ALS patients and controls.[1]

Biomarkers		ALS	Healthy	CNS	Periphery
PPIA, sol	N	79	104	63	48
	Median	73.3	117.3	85.7	102.9
	OR (95% CI)	1	1.35 (1.23-1.48)	1.14 (1.03-1.25)	1.18 (1.07-1.31)
	P value	< 0.001			
	AUC (95% CI)	-	**0.79 (0.73-0.86)**	0.59 (0.49-0.68)	**0.71 (0.62-0.80)**
HSC70, sol	N	73	77	59	47
	Median	82.7	52.8	57.3	88.0
	OR (95% CI)	1	0.87 (0.81-0.93)	0.92 (0.86-0.98)	1.00 (0.95-1.05)
	P value	< 0.001			
	AUC (95% CI)	-	0.69 (0.60-0.77)	0.63 (0.53-0.73)	0.49 (0.38-0.59)
TDP-43, sol	N	78	99	62	48
	Median	96.5	99.7	95.7	137.3
	OR (95% CI)	1	1.00 (0.96-1.05)	1.03 (0.98-1.08)	1.08 (1.02-1.14)
	P value	0.012			
	AUC (95% CI)	-	0.51 (0.42-0.59)	0.52 (0.42-0.62)	0.66 (0.56-0.75)
hnRNPA2B1, sol	N	89	101	63	48
	Median	90.4	100.1	117.1	130.3
	OR (95% CI)	1	1.06 (0.99-1.13)	1.16 (1.09-1.24)	1.20 (1.11-1.28)
	P value	< 0.001			
	AUC (95% CI)	-	0.57 (0.49-0.65)	0.67 (0.58-0.76)	**0.73 (0.64-0.82)**
SOD1, sol	N	63	56	53	41
	Median	81.1	70.3	69.6	145.8
	OR (95% CI)	1	0.97 (0.93-1.01)	1.00 (0.97-1.03)	1.05 (1.01-1.09)
	P value	0.002			
	AUC (95% CI)	-	0.61 (0.50-0.71)	0.51 (0.41-0.62)	**0.76 (0.66-0.85)**
PPIA, ins	N	88	98	61	47
	Median	87.0	43.9	95.6	83.3
	OR (95% CI)	1	0.81 (0.74-0.88)	1.06 (0.97-1.15)	0.98 (0.89-1.07)
	P value	< 0.001			
	AUC (95% CI)	-	**0.72 (0.64-0.79)**	0.57 (0.48-0.66)	0.52 (0.42-0.62)
HSC70, ins	N	85	58	59	46
	Median	77.3	59.0	92.6	74.4
	OR (95% CI)	1	0.83 (0.71-0.97)	1.20 (1.04-1.39)	0.93 (0.79-1.09)
	P value	0.001			
	AUC (95% CI)	-	0.64 (0.54-0.75)	0.65 (0.55-0.75)	0.55 (0.43-0.66)
TDP-43, ins	N	79	76	56	42
	Median	50.3	25.0	68.3	72.1
	OR (95% CI)	1	0.68 (0.58-0.79)	1.15 (1.05-1.26)	1.18 (1.08-1.30)
	P value	< 0.001			
	AUC (95% CI)	-	**0.76 (0.69-0.84)**	0.65 (0.56-0.75)	0.63 (0.52-0.75)
hnRNPA2B1, ins	N	85	58	59	46
	Median	156.7	83.7	131.7	140.8
	OR (95% CI)	1	0.93 (0.89-0.96)	0.98 (0.95-1.01)	0.97 (0.94-1.00)
	P value	0.002			
	AUC (95% CI)	-	0.68 (0.59-0.77)	0.53 (0.43-0.62)	0.55 (0.45-0.65)
SOD1, ins	N	79	45	52	39
	Median	63.1	47.3	91.9	88.0
	OR (95% CI)	1	0.87 (0.78-0.98)	1.16 (1.06-1.28)	1.13 (1.03-1.24)
	P value	< 0.001			
	AUC (95% CI)	-	0.62 (0.52-0.70)	**0.70 (0.61-0.79)**	0.67 (0.57-0.77)
Insolubility index	N	91	94	65	49
	Median	1.46	0.84	1.13	0.90
	OR (95% CI)	1	0.83 (0.72-0.96)	0.98 (0.88-1.09)	0.73 (0.57-0.94)
	P value	0.013			
	AUC (95% CI)	-	0.65 (0.57-0.73)	0.56 (0.47-0.65)	0.69 (0.60-0.77)

[1] OR: odds ratio. All ORs are associated with a 10-A.U. increase in biomarker levels except for the insolubility index, associated with a 1-A.U. increase. The AUC values ≥ 0.7 are bold highlighted; Sol, soluble; Ins, insoluble.

in the four groups by univariate analysis and multivariate analysis, adjusting for age and sex (Table 2, Supplementary Table 1). Insoluble PPIA, TDP-43 and hnRNPA2B1 were higher in ALS patients than in Healthy controls, while HSC70 was not significantly different. Insoluble TDP-43 was also significantly lower in ALS than in CNS and Periphery controls. When we stratified ALS patients according to the rate of disease progression, there was a progressively higher level of insoluble hnRNPA2B1 as the rate of disease progression rose (Fig. 4E), which is consistent with the opposite trend in the soluble fraction (Fig. 2E). No difference was found for PPIA, HSC70, TDP-43 in ALS patients with different disease progression rates (data not shown).

3.4. Combinations of PBMC biochemical parameters distinguish ALS from controls with high accuracy

We assessed the diagnostic values of the PBMC biochemical parameters by ROC curve analysis. Six of the 11 parameters reached an AUC equal to or greater than 0.70 (Supplementary Table 1), which corresponds to moderate discriminatory power. PPIA, soluble and insoluble, and TDP-43 insoluble distinguished ALS patients from healthy subjects, SOD1 insoluble ALS patients from CNS controls, PPIA soluble, hnRNPA2B1 soluble, SOD1 soluble ALS patients from Periphery controls. When combinations of parameters were considered, the discriminatory power was greater (Fig. 5A–C). Multivariate analysis identified PPIA soluble and hnRNPA2B1 insoluble as the combination

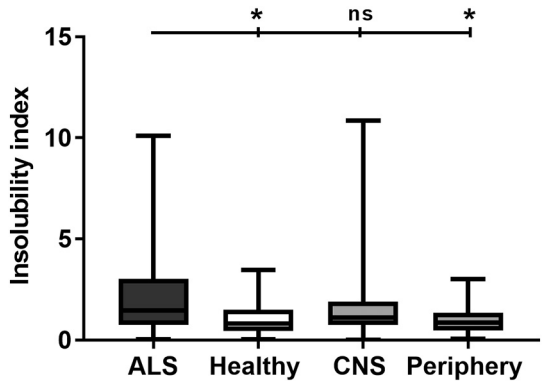

Fig. 3. An index of insolubility was calculated for all PBMC samples in the analysis. PBMC samples were from ALS patients (n = 93), healthy subjects (n = 104), CNS controls (CNS) (n = 63) or Periphery controls (Periphery) (n = 48). Box plots indicate the ratio of the amount of protein in PBMC-insoluble to that in PBMC-soluble. The insolubility index was distributed differently in the four groups (Table 2). *, different from ALS ($p < 0.05$); ns, not significantly different from ALS.

of parameters with the best discriminatory power for distinguishing ALS patients from Healthy controls (AUC 0.85; 95% CI: 0.79-0.90). For this combination the optimal cut-off generated 74% sensitivity and 76% specificity, providing a correct classification in 77% of the cases. PPIA soluble, TDP-43 insoluble and hnRNPA2B1 soluble was the combination of parameters with the best discriminatory power for distinguishing ALS patients from CNS (AUC 0.75; 95% CI: 0.65-0.82) and Periphery controls (AUC 0.82; 95% CI: 0.73-0.88). This combination distinguished ALS patients from CNS controls with 72% sensitivity and 60% specificity, providing a correct classification in 67% of the cases, and ALS patients from Periphery controls with 83% sensitivity and 69% specificity, providing a correct classification in 75% of the cases.

3.5. PPIA soluble has prognostic potential

We analyzed the correlations between the PBMC biochemical parameters and the clinical variables of ALS patients, such as disease severity (ALSFRS-R score), rate of disease progression (ΔALSFRS-R), symptom duration at sampling, and disease duration (from sampling to death or tracheostomy) (Fig. 6, Table 3). There was a significant, though weak, association between PPIA soluble or hnRNPA2B1insoluble and ALSFRS-R score (Fig. 6A–B), and a moderate association between TDP-43 insoluble ($r = 0.513$, $p < 0.001$) or SOD1 insoluble ($r = 0.349$, $p = 0.001$) and symptom duration at sampling (Fig. 6C–D). We analyzed the correlation between the biomarkers and disease duration in 66 out of 93 ALS patients (68%). After a median (interquartile range) follow-up of 66.2 (57.8-78.5) months 61 were deceased (92%). ALS patients had a median (95% CI) disease duration of 14.5 (9.5-17.4) months. Table 3 shows that PPIA soluble was the biochemical parameter best explaining the prognosis, suggesting that high PPIA soluble levels are associated with a lower risk of mortality (hazard ratio

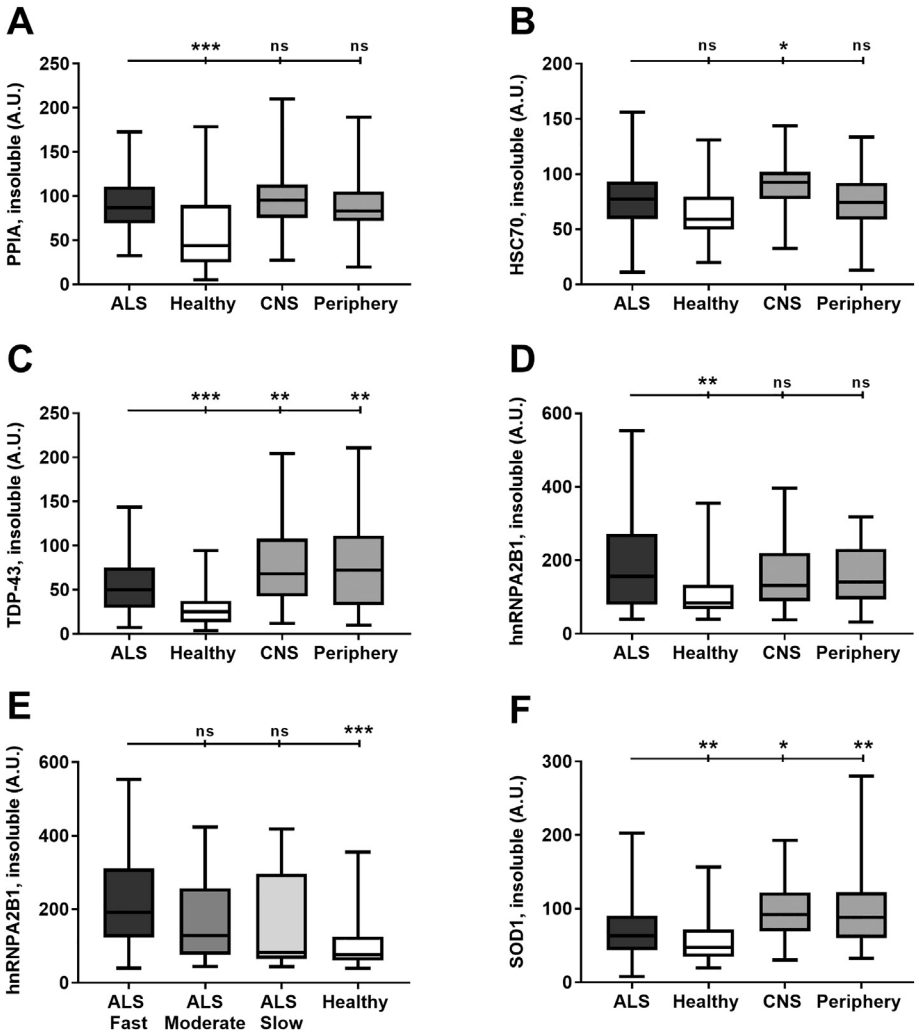

Fig. 4. Analysis of candidate biomarkers in PBMC-insoluble from ALS patients and controls. (A–F) PPIA, HSC70, TDP-43, hnRNPA2B1 and SOD1 were analyzed by slot blot analysis in PBMC-insoluble from ALS patients (n = 93), healthy subjects (n = 104), CNS controls (CNS) (n = 63) or Periphery controls (Periphery) (n = 48). (E) The levels of hnRNPA2B1 in ALS patients, stratified by rate of disease progression as fast, moderate or slow, were compared with those in Healthy controls. Box plots indicate immunoreactivity normalized to total protein loading and to the internal standard, in arbitrary units (A.U.). In all cases the proteins were distributed differently in the four groups (Table 2). Protein levels different from ALS (A–D, F) or fast ALS (E), with $p < 0.05$ (*), $p < 0.01$ (**), $p < 0.001$ (***); ns, not significantly different from ALS (A–D, F) or fast ALS (E).

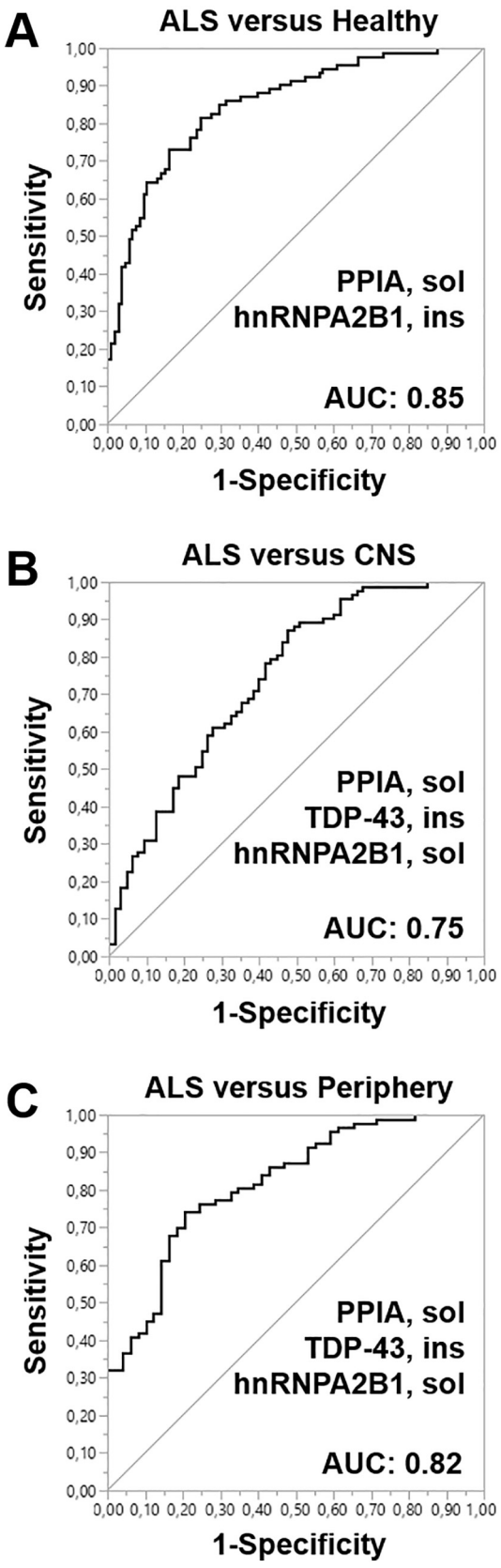

Fig. 5. ROC curves and AUC for the combination of PBMC biochemical parameters with the highest discriminatory power for distinguishing ALS from Healthy subjects (A), CNS controls (B), Periphery controls (C).

[HR] 0.94 [95% CI: 0.85-1.03]). The point estimate was confirmed (HR 0.92 [95% CI: 0.83-1.01]) adjusting for factors known to be associated with survival, such as site of onset, age at symptom onset, and sex. The unsatisfactory p value might be explained by the few death events collected, unbalanced unknown confounding factors and assumption of normality not satisfied by biomarker distribution. We next stratified patients for high or low levels of PPIA soluble, using the median PPIA soluble level as cut-off. Kaplan-Meier curves for disease duration of ALS patients with high or low levels of PPIA soluble separated markedly, with a median disease duration 5.7 months shorter for ALS patients with low PPIA soluble levels (Fig. 6E), suggesting that PPIA soluble has prognostic value.

4. Discussion

For ALS there is no effective disease-modifying therapy. Heterogeneity and lack of specific biomarkers for early diagnosis, patient stratification and monitoring is a major limitation to the development of therapy. Easily accessible clinical samples and reliable analytical methods are fundamental for the development of biomarkers for clinical use. In this study we investigated a panel of PBMC proteins in their soluble and relatively insoluble forms in a large, well-characterized cohort of ALS patients and controls. We established a cost-effective, highly controlled analytical procedure, permitting replication studies. We found that combinations of biochemical parameters in PBMC could distinguish ALS patients from controls with high accuracy, and PPIA has promising prognostic value.

There is now compelling evidence that immune dysregulation can both initiate and contribute to the pathogenesis of ALS (Beers and Appel, 2019). ALS patients have alterations in the immune system. For example, peripheral monocytes have a pro-inflammatory phenotype (Butovsky et al., 2012), and dysfunctional regulatory T lymphocytes correlate with the extent and rapidity of the disease (Henkel et al., 2013). There is also evidence that PBMCs might be a useful source of protein biomarkers for ALS (Nardo et al., 2011; Filareti et al., 2017; De Marco et al., 2011; Mougeot et al., 2011; De Marco et al., 2017). In two previous exploratory studies we found significant changes in the PBMC protein profile of ALS patients compared to control subjects (Nardo et al., 2011; Filareti et al., 2017). The aim of the present study was to investigate further a number of selected proteins in PBMC samples from a larger cohort of sporadic ALS patients and controls. We selected PPIA, HSC70, TDP-43 and hnRNPA2B1 as candidate protein biomarkers because they are involved in protein (PPIA, HSC70) and RNA (TDP-43 and hnRNPA2B1) homeostasis, extremely important intersecting pathways that if impaired may cause ALS (Alberti and Carra, 2018; Ling et al., 2013). In contrast with NFs in biological fluids, the selected PBMC proteins are abundantly expressed and do not need sophisticated analytical methods. However, their particular biochemical characteristics call for highly controlled processing procedures to provide consistent data in a large clinical study. They were all enriched in detergent-insoluble fractions isolated from spinal cord of the mutant SOD1 mouse and post-mortem tissues of ALS patients (Lauranzano et al., 2015; Basso et al., 2009; Seyfried et al., 2012). *In vitro*, under stress conditions, PPIA, HSC70, hnRNPA2B1 and TDP-43 were associated with stress granules or granule-like structures in the cytoplasm (Ivanova et al., 2015; Xiang et al., 2015; Buchan and Parker, 2009). They contain a low-complexity domain (TDP-43 and hnRNPA2B1) or have affinity for it (PPIA) (Lauranzano et al., 2015), which may polymerize into amyloid-like fibers (Kato et al., 2012). Besides this panel of proteins, we analyzed SOD1 which, even without the mutation, may acquire a misfolded structure and form aggregates in brain, spinal cord and PBMCs of sporadic ALS patients (Cereda et al., 2013; Paré et al., 2018; Bosco et al., 2010; Forsberg et al., 2010). Moreover, misfolded SOD1, similarly to TDP-43 and other RNA-binding proteins, have a tendency to accumulate and aggregate within stress granules in human cells (Mateju et al., 2017).

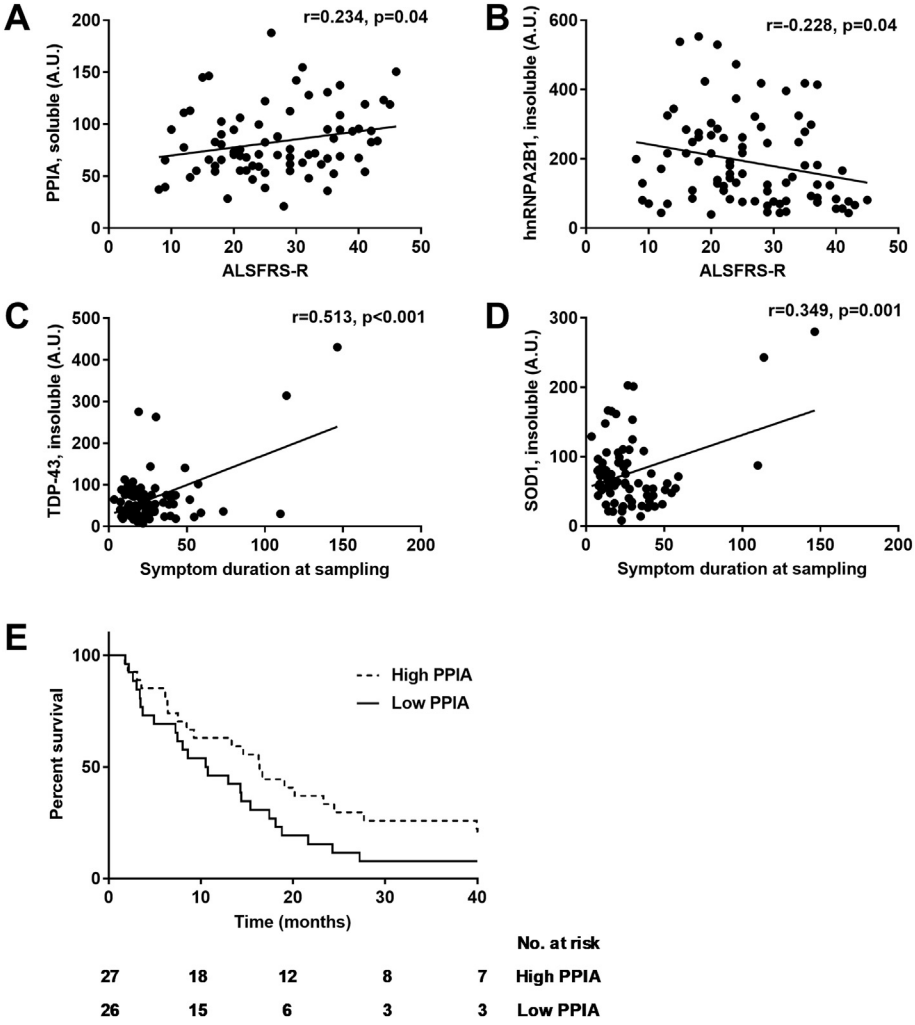

Fig. 6. Correlation analyses of PPIA soluble or hnRNPA2B1 insoluble levels with ALSFRS-R (A–B), and TDP-43 insoluble or SOD1 insoluble levels with symptom duration at sampling (months) (C–D); (E) Kaplan-Meier curves for survival (time in months from sampling to death or tracheostomy) of ALS patients with high or low levels of PPIA soluble, and number of subjects at risk.

Table 3
Univariate analysis for evaluating association of PBMC biochemical parameters and disease duration in ALS patients.

Biomarkers	HR[1]	P-value	Cut-off[2]	Survival/high[3]	Survival/low[3]	HR[4]
PPIA, sol	0.94 (0.85-1.03)	0.17	74.5 (21.0-188.0)	16.4 (0.9-2.7)	10.6 (0.4-1.1)	0.92 (0.83-1.01)
HSC70, sol	1.01 (0.97-1.04)	0.70	82.6 (6.7-11.0)	11.8 (0.5-1.5)	14.3 (0.7-2.2)	0.99 (0.96-1.03)
TDP-43, sol	1.00 (0.97-1.03)	0.88	97.8 (20.8-394.2)	14.4 (0.6-1.7)	14.8 (0.6-1.8)	0.99 (0.96-1.02)
hnRNPA2B1, sol	1.04 (0.99-1.09)	0.11	91.0 (2.6-319.8)	14.4 (0.6-1.6)	14.6 (0.6-1.7)	1.00 (0.99-1.01)
SOD1, sol	1.01 (0.99-1.02)	0.36	81.6 (36.9-959.6)	15.0 (0.8-3.6)	8.9 (0.3-1.3)	1.00 (0.98-1.02)
PPIA, ins	1.00 (0.93-1.08)	0.95	52.1 (7.1-430.8)	12.0 (0.4-1.3)	16.0 (0.8-2.3)	1.03 (0.95-1.12)
HSC70, ins	0.96 (0.87-1.06)	0.45	77.7 (11.0-156.3)	14.9 (0.6-1.7)	15.2 (0.6-1.8)	0.97 (0.88-1.07)
TDP-43, ins	1.01 (0.98-1.04)	0.61	52.1 (7.1-430.8)	11.1 (0.4-1.2)	16.3 (0.8-2.5)	1.01 (0.98-1.04)
hnRNPA2B1, ins	1.02 (1.00-1.04)	0.09	156.8 (39.8-553.4)	13.3 (0.4-1.3)	17.8 (0.8-2.6)	1.02 (0.99-1.04)
SOD1, ins	1.02 (0.98-1.06)	0.33	63.2 (7.8-280.2)	11.4 (0.4-1.2)	16.3 (0.8-2.4)	1.01 (0.97-1.06)
Insolubility index	0.92 (0.79-1.08)	0.33	1.0 (0.03-8.8)	14.4 (0.6-1.6)	14.6 (0.6-1.8)	0.96 (0.82-1.13)

[1] HR: HRs (95% CI) by univariate Cox regression model. HRs are associated with a 10-A.U. increase in biomarker levels except for the insolubility index which is associated with a 1-A.U. increase.

[2] Cut-off: the median (range) biomarker level in A.U. used as cut-off for stratification in sub-groups of ALS patients with high or low levels of biomarkers.

[3] Survival/high or /low: median (95% CI) survival (time in months from sampling to death or tracheostomy) of ALS patients stratified for high or low levels of biomarkers.

[4] HR, HRs (95% CI) adjusted for site of onset, age at symptom onset and sex; Sol, soluble; Ins, insoluble.

PBMC proteins were extracted by a differential detergent fractionation method that leads to separation of the PBMC-soluble and PBMC-insoluble fractions. We calculated the insolubility index for each sample to assess whether the protein partitioning changed in the different clinical conditions. Interestingly, insolubility was higher in all pathological conditions than in Healthy controls, and highest in ALS, indicating that this biochemical parameter may unmask ALS-specific features. The proteins enriched in the insoluble fraction cannot be truly

considered protein aggregates since no general increase in ubiquitination was detected. Instead, in all pathological conditions there was enrichment in the markers of stress granules, such as TIA1 and G3BP1 (Jain et al., 2016), in hnRNPA2B1 and TDP -43, RNP granule components, and in the 35 KDa TDP-43 fragment, recruited to stress granules under chronic oxidative stress (Meyerowitz et al., 2011). There was also enrichment in SQSTM1/p62, which is implicated in stress granule targeting for autophagic degradation, also in an ubiquitin-independent manner (Chitiprolu et al., 2018). We therefore favor the hypothesis that the insoluble fraction is enriched in supramolecular assemblies and membraneless organelles, including stress granules, that accumulate in pathological conditions.

The single biochemical parameters were not able to distinguish accurately ALS patients from controls. However, this is not surprising, given the complexity and heterogeneity of the disease, as noted in our previous study (Nardo et al., 2011). Multiple biomarker combinations are also used in Alzheimer's disease to predict dementia in people with mild cognitive impairment (Jack et al., 2018). The combinations of biomarkers accurately distinguished ALS patients from Healthy and Periphery controls, but performed less well for CNS controls, reflecting overlapping pathological features between ALS and diseases affecting the CNS, which are also detectable in PBMCs. For example, brain deposition of TDP-43 is in different diseases, associated or not with neurodegeneration (Hatsuta et al., 2019; Smith et al., 2019; Pasanen et al., 2014; Yokota et al., 2010; Yang et al., 2018), such as stroke, progressive supranuclear palsy, Parkinson's disease, that are included in our control CNS group. It would now be interesting to see whether the biomarker signatures identified in ALS PBMCs are already detectable at a presymptomatic stage of the disease. Chiò's group detected mislocalized TDP-43 in PBMCs in three neurologically unaffected individuals carrying the familial TARDBP mutation (De Marco et al., 2011; De Marco et al., 2017). Changes in PPIA levels were found in PBMCs of the $SOD1^{G93A}$ rat model of ALS already at a presymptomatic stage (Nardo et al., 2011). This evidence suggests that at least TDP-43 and PPIA, the most significant parameters distinguishing ALS patients from healthy controls, might be useful to identify subjects at risk of disease in the absence of clinical symptoms.

In ALS patients there was a shift toward greater partitioning in the PBMC-insoluble than control condition for the bulk of the proteins, but in particular for PPIA, TDP-43 and hnRNPA2B1. This shift, which consists in a lower soluble level and/or a higher insoluble level of these proteins, correlates with a worse disease phenotype in ALS patients, such as greater severity, for PPIA and hnRNPA2B1, faster progression for hnRNPA2B1, and earlier death for PPIA. Hypothetically, under pathological conditions these proteins change their biochemical properties, quite likely through post-translational modifications, and engage in common pathogenic mechanisms, pointing to additional hints for therapies. PPIA undergoes a number of post-translational modifications (Lauranzano et al., 2015; Ghezzi et al., 2006; Massignan et al., 2007) that may be at the basis of its change in partitioning, interaction partners and functions. In the spinal cord of the mutant SOD1 mouse, PPIA already changes its post-translational pattern at a presymptomatic stage of the disease (Massignan et al., 2007). In PBMCs of ALS patients, PPIA is less Lys-acetylated than in controls, a modification necessary for PPIA to interact with TDP-43 (Lauranzano et al., 2015). The fact that a low level of soluble PPIA correlates with earlier death may be linked to a lack of PPIA key protective functions in the cells, since it is a foldase and a molecular chaperone with antioxidant activity (Fischer et al., 1989; Freskgård et al., 1992; Choi et al., 2007; Doyle et al., 1999). The absence of PPIA exacerbated TDP-43 and SOD1 aggregation and accelerated disease progression in the mutant SOD1 mouse model (Lauranzano et al., 2015). More recently, we observed that mice knockout for PPIA, without mutant SOD1, develop a neuropathological phenotype with aging (Pasetto et al., manuscript submitted). Finally, low levels of PPIA in PBMCs of ALS patients are associated with an early disease onset (Filareti et al., 2017). Thus, all these pieces of evidence indicate that PPIA is a disease modifier, with interesting prognostic potential.

ALS patients display widely differing patterns of disease manifestation and progression (Beghi et al., 2011). This heterogeneity causes problems for clinical trial interpretation and care. Stratifying ALS patients in homogenous sub-groups could be useful for developing effective and more personalized treatments, especially in cases with an unknown genetic link. Panels of biomarkers will probably be needed to stratify patients and detect changes over a short period. Validation on longitudinal cohorts is now necessary to see whether these PBMC biomarkers can be used to monitor disease progression and/or efficacy in clinical trials, with immune dysregulation/protein and RNA homeostasis mechanisms as the therapeutic targets. A good opportunity is offered by the ongoing phase II clinical trial on RNS60 (NCT03456882), a compound that has shown a therapeutic effect in the mutant SOD1 mouse model through protective glial and immune cells (Vallarola et al., 2018), and long-term treatment was safe and well tolerated in ALS patients (Paganoni et al., 2019). The effect of RNS60 on a panel of exploratory pharmacodynamic biomarkers in PBMCs, including PPIA, will be examined and possibly validate the use of PPIA to stratify patients.

In conclusion, PBMC proteins indicative of changes in protein and RNA homeostasis, that may underlie membraneless organelle formation, are promising biomarkers of ALS, for diagnosis, prognosis and patient stratification. Additional studies are needed to establish their clinical use.

Funding sources

This work was supported by grants from the European Community's Seventh Framework Programme (FP7/2007-2013) under grant agreement Euro-MOTOR (no. 259867) (to V.B.), the Italian Ministry of Health, Ricerca Finalizzata 2010 project 2313991 (to G.M., C.L. and V.B.) and Ricerca Finalizzata 2018 project 12365614 (to V.B.), the "Fondazione Regionale per la Ricerca Biomedica di Regione Lombardia", project TRANS-ALS (to V.B.), and Intesa San Paolo S.p.A., project no. B/2018/0061 (to V.B.).

Declaration of Competing Interest

The authors declare no competing interests.

Acknowledgements

We are grateful to Silvia Pozzi, Eliana Lauranzano, Mauro Pignataro, Riccardo Stucchi, Mariachiara Castelnovo, Katia Paolella, Melissa Mombrini, Valeria Giannone, Lorena Cucci, Francesca Stella, Mattia Dominici, Serena Scozzari for help in processing PBMC samples; Elisabetta Pupillo and Ettore Beghi for help in recruiting control subjects; Riccardo Sideri and Francesca Gerardi for help in collecting patient data. We thank Judith Baggott for editorial assistance.

Appendix A. Supplementary data

Supplementary data to this article can be found online at https://doi.org/10.1016/j.nbd.2020.104815.

References

Alberti, S., Carra, S., 2018. Quality control of membraneless organelles. J. Mol. Biol. 430, 4711–4729. https://doi.org/10.1016/j.jmb.2018.05.013.

Basso, M., Samengo, G., Nardo, G., Massignan, T., D'Alessandro, G., Tartari, S., et al., 2009. Characterization of detergent-insoluble proteins in ALS indicates a causal link between nitrative stress and aggregation in pathogenesis. PLoS One 4, e8130. https://doi.org/10.1371/journal.pone.0008130.

Beers, D.R., Appel, S.H., 2019. Immune dysregulation in amyotrophic lateral sclerosis: mechanisms and emerging therapies. Lancet Neurol. 18, 211–220. https://doi.org/

10.1016/S1474-4422(18)30394-6.
Beghi, E., Chio, A., Couratier, P., Esteban, J., Hardiman, O., Logroscino, G., et al., 2011. The epidemiology and treatment of ALS: focus on the heterogeneity of the disease and critical appraisal of therapeutic trials. Amyotroph. Lateral Scler. 12, 1–10. https://doi.org/10.3109/17482968.2010.502940.
Benatar, M., Wuu, J., Andersen, P.M., Lombardi, V., Malaspina, A., 2018. Neurofilament light: a candidate biomarker of pre-symptomatic ALS and phenoconversion. Ann. Neurol. https://doi.org/10.1002/ana.25276.
Bosco, D.A., Morfini, G., Karabacak, N.M., Song, Y., Gros-Louis, F., Pasinelli, P., et al., 2010. Wild-type and mutant SOD1 share an aberrant conformation and a common pathogenic pathway in ALS. Nat. Neurosci. 13, 1396–1403. https://doi.org/10.1038/nn.2660.
Brooks, B.R., Miller, R.G., Swash, M., Munsat, T.L., 2000. El Escorial revisited: revised criteria for the diagnosis of amyotrophic lateral sclerosis. Amyotroph. Lateral Scler. Mot. Neuron Disord. 1, 293–299.
Buchan, J.R., Parker, R., 2009. Eukaryotic stress granules: the ins and outs of translation. Mol. Cell 36, 932–941. https://doi.org/10.1016/j.molcel.2009.11.020.
Butovsky, O., Siddiqui, S., Gabriely, G., Lanser, A.J., Dake, B., Murugaiyan, G., et al., 2012. Modulating inflammatory monocytes with a unique microRNA gene signature ameliorates murine ALS. J. Clin. Invest. 122, 3063–3087. https://doi.org/10.1172/JCI62636.
Calini, D., Corrado, L., Del Bo, R., Gagliardi, S., Pensato, V., Verde, F., et al., 2013. Analysis of hnRNPA1, A2/B1, and A3 genes in patients with amyotrophic lateral sclerosis. Neurobiol. Aging 34https://doi.org/10.1016/j.neurobiolaging.2013.05.025. (2695.e11-12).
Cereda, C., Leoni, E., Milani, P., Pansarasa, O., Mazzini, G., Guareschi, S., et al., 2013. Altered intracellular localization of SOD1 in leukocytes from patients with sporadic amyotrophic lateral sclerosis. PLoS One 8, e75916. https://doi.org/10.1371/journal.pone.0075916.
Chio, A., Logroscino, G., Hardiman, O., Swingler, R., Mitchell, D., Beghi, E., et al., 2008. Prognostic factors in ALS: a critical review. Amyotroph. Lateral Scler. 1–14. https://doi.org/10.1080/17482960802566824.
Chipika, R.H., Finegan, E., Li Hi Shing, S., Hardiman, O., Bede, P., 2019. Tracking a fast-moving disease: longitudinal markers, monitoring, and clinical trial endpoints in ALS. Front. Neurol. 10. https://doi.org/10.3389/fneur.2019.00229.
Chitiprolu, M., Jagow, C., Tremblay, V., Bondy-Chorney, E., Paris, G., Savard, A., et al., 2018. A complex of C9ORF72 and p62 uses arginine methylation to eliminate stress granules by autophagy. Nat. Commun. 9, 2794. https://doi.org/10.1038/s41467-018-05273-7.
Choi, K.J., Piao, Y.J., Lim, M.J., Kim, J.H., Ha, J., Choe, W., et al., 2007. Overexpressed cyclophilin A in cancer cells renders resistance to hypoxia- and cisplatin-induced cell death. Cancer Res. 67, 3654–3662. https://doi.org/10.1158/0008-5472.CAN-06-1759.
De Marco, G., Lomartire, A., Calvo, A., Risso, A., De Luca, E., Mostert, M., et al., 2017. Monocytes of patients with amyotrophic lateral sclerosis linked to gene mutations display altered TDP-43 subcellular distribution. Neuropathol. Appl. Neurobiol. 43, 133–153. https://doi.org/10.1111/nan.12328.
De Marco, G., Lupino, E., Calvo, A., Moglia, C., Buccinna, B., Grifoni, S., et al., 2011. Cytoplasmic accumulation of TDP-43 in circulating lymphomonocytes of ALS patients with and without TARDBP mutations. Acta Neuropathol. 121, 611–622. https://doi.org/10.1007/s00401-010-0786-7.
De Schaepdryver, M., Goossens, J., De Meyer, S., Jeromin, A., Masrori, P., Brix, B., et al., 2019. Serum neurofilament heavy chains as early marker of motor neuron degeneration. Ann. Clin. Transl. Neurol. https://doi.org/10.1002/acn3.50890.
Disanto, G., Barro, C., Benkert, P., Naegelin, Y., Schädelin, S., Giardiello, A., et al., 2017. Serum neurofilament light: a biomarker of neuronal damage in multiple sclerosis. Ann. Neurol. 81, 857–870. https://doi.org/10.1002/ana.24954.
Doyle, V., Virji, S., Crompton, M., 1999. Evidence that cyclophilin-A protects cells against oxidative stress. Biochem. J. 341 (Pt 1), 127–132.
Fang, M.Y., Markmiller, S., Vu, A.Q., Javaherian, A., Dowdle, W.E., Jolivet, P., et al., 2019. Small-molecule modulation of TDP-43 recruitment to stress granules prevents persistent TDP-43 accumulation in ALS/FTD. Neuron 103https://doi.org/10.1016/j.neuron.2019.05.048. (802–819.e11).
Feneberg, E., Oeckl, P., Steinacker, P., Verde, F., Barro, C., Van Damme, P., et al., 2018. Multicenter evaluation of neurofilaments in early symptom onset amyotrophic lateral sclerosis. Neurology 90, e22–e30. https://doi.org/10.1212/WNL.0000000000004761.
Filareti, M., Luotti, S., Pasetto, L., Pignataro, M., Paolella, K., Messina, P., et al., 2017. Decreased levels of foldase and chaperone proteins are associated with an early-onset amyotrophic lateral sclerosis. Front. Mol. Neurosci. 10, 99. https://doi.org/10.3389/fnmol.2017.00099.
Fischer, G., Wittmann-Liebold, B., Lang, K., Kiefhaber, T., Schmid, F.X., 1989. Cyclophilin and peptidyl-prolyl cis-trans isomerase are probably identical proteins. Nature 337, 476–478. https://doi.org/10.1038/337476a0.
Forsberg, K., Jonsson, P.A., Andersen, P.M., Bergemalm, D., Graffmo, K.S., Hultdin, M., et al., 2010. Novel antibodies reveal inclusions containing non-native SOD1 in sporadic ALS patients. PLoS One 5, e11552. https://doi.org/10.1371/journal.pone.0011552.
Freskgård, P.O., Bergenhem, N., Jonsson, B.H., Svensson, M., Carlsson, U., 1992. Isomerase and chaperone activity of prolyl isomerase in the folding of carbonic anhydrase. Science 258, 466–468.
Ghezzi, P., Casagrande, S., Massignan, T., Basso, M., Bellacchio, E., Mollica, L., et al., 2006. Redox regulation of cyclophilin A by glutathionylation. Proteomics 6, 817–825. https://doi.org/10.1002/pmic.200500177.
Hatsuta, H., Takao, M., Nogami, A., Uchino, A., Sumikura, H., Takata, T., et al., 2019. Tau and TDP-43 accumulation of the basal nucleus of Meynert in individuals with cerebral lobar infarcts or hemorrhage. Acta Neuropathol. Commun. 7, 49. https://doi.org/10.1186/s40478-019-0700-z.
Henkel, J.S., Beers, D.R., Wen, S., Rivera, A.L., Toennis, K.M., Appel, J.E., et al., 2013. Regulatory T-lymphocytes mediate amyotrophic lateral sclerosis progression and survival. EMBO Mol. Med. 5, 64–79. https://doi.org/10.1002/emmm.201201544.
Ilieva, H., Polymenidou, M., Cleveland, D.W., 2009. Non-cell autonomous toxicity in neurodegenerative disorders: ALS and beyond. J. Cell Biol. 187, 761–772. https://doi.org/10.1083/jcb.200908164.
Ivanova, A.A., Velichko, A.K., Kantidze, O.L., Razin, S.V., 2015. Heat stress induces formation of cytoplasmic granules containing HSC70 protein. Dokl. Biochem. Biophys. 463, 213–215. https://doi.org/10.1134/S1607672915040043.
Jack, C.R., Bennett, D.A., Blennow, K., Carrillo, M.C., Dunn, B., Haeberlein, S.B., et al., 2018. NIA-AA research framework: toward a biological definition of Alzheimer's disease. Alzheimers Dement J. Alzheimers Assoc. 14, 535–562. https://doi.org/10.1016/j.jalz.2018.02.018.
Jain, S., Wheeler, J.R., Walters, R.W., Agrawal, A., Barsic, A., Parker, R., 2016. ATPase-modulated stress granules contain a diverse proteome and substructure. Cell 164, 487–498. https://doi.org/10.1016/j.cell.2015.12.038.
Kato, M., Han, T.W., Xie, S., Shi, K., Du, X., Wu, L.C., et al., 2012. Cell-free formation of RNA granules: low complexity sequence domains form dynamic fibers within hydrogels. Cell 149, 753–767. https://doi.org/10.1016/j.cell.2012.04.017.
Khalil, M., Teunissen, C.E., Otto, M., Piehl, F., Sormani, M.P., Gattringer, T., et al., 2018. Neurofilaments as biomarkers in neurological disorders. Nat. Rev. Neurol. 14, 577–589. https://doi.org/10.1038/s41582-018-0058-z.
Kim, H.J., Kim, N.C., Wang, Y.D., Scarborough, E.A., Moore, J., Diaz, Z., et al., 2013. Mutations in prion-like domains in hnRNPA2B1 and hnRNPA1 cause multisystem proteinopathy and ALS. Nature 495, 467–473. https://doi.org/10.1038/nature11922.
Kimura, F., Fujimura, C., Ishida, S., Nakajima, H., Furutama, D., Uehara, H., et al., 2006. Progression rate of ALSFRS-R at time of diagnosis predicts survival time in ALS. Neurology 66, 265–267. https://doi.org/10.1212/01.wnl.0000194316.91908.8a.
Lagier-Tourenne, C., Polymenidou, M., Cleveland, D.W., 2010. TDP-43 and FUS/TLS: emerging roles in RNA processing and neurodegeneration. Hum. Mol. Genet. https://doi.org/10.1093/hmg/ddq137.
Lauranzano, E., Pozzi, S., Pasetto, L., Stucchi, R., Massignan, T., Paolella, K., et al., 2015. Peptidylprolyl isomerase A governs TARDBP function and assembly in heterogeneous nuclear ribonucleoprotein complexes. Brain 138, 974–991. https://doi.org/10.1093/brain/awv005.
Ling, S.C., Polymenidou, M., Cleveland, D.W., 2013. Converging mechanisms in ALS and FTD: disrupted RNA and protein homeostasis. Neuron 79, 416–438. https://doi.org/10.1016/j.neuron.2013.07.033.
Liu, T., Daniels, C.K., Cao, S., 2012. Comprehensive review on the HSC70 functions, interactions with related molecules and involvement in clinical diseases and therapeutic potential. Pharmacol. Ther. 136, 354–374. https://doi.org/10.1016/j.pharmthera.2012.08.014.
Massignan, T., Casoni, F., Basso, M., Stefanazzi, P., Biasini, E., Tortarolo, M., et al., 2007. Proteomic analysis of spinal cord of presymptomatic amyotrophic lateral sclerosis G93A SOD1 mouse. Biochem. Biophys. Res. Commun. 353, 719–725. https://doi.org/10.1016/j.bbrc.2006.12.075.
Mateju, D., Franzmann, T.M., Patel, A., Kopach, A., Boczek, E.E., Maharana, S., et al., 2017. An aberrant phase transition of stress granules triggered by misfolded protein and prevented by chaperone function. EMBO J. 36, 1669–1687. https://doi.org/10.15252/embj.201695957.
Meyerowitz, J., Parker, S.J., Vella, L.J., Ng, D.C., Price, K.A., Liddell, J.R., et al., 2011. C-Jun N-terminal kinase controls TDP-43 accumulation in stress granules induced by oxidative stress. Mol. Neurodegener. 6, 57. https://doi.org/10.1186/1750-1326-6-57.
Mougeot, J.-L.C., Li, Z., Price, A.E., Wright, F.A., Brooks, B.R., 2011. Microarray analysis of peripheral blood lymphocytes from ALS patients and the SAFE detection of the KEGG ALS pathway. BMC Med. Genet. 4. https://doi.org/10.1186/1755-8794-4-74.
Nardo, G., Pozzi, S., Pignataro, M., Lauranzano, E., Spano, G., Garbelli, S., et al., 2011. Amyotrophic lateral sclerosis multiprotein biomarkers in peripheral blood mononuclear cells. PLoS One 6, e25545. https://doi.org/10.1371/journal.pone.0025545.
Paganoni, S., Alshikho, M.J., Luppino, S., Chan, J., Pothier, L., Schoenfeld, D., et al., 2019. A pilot trial of RNS60 in amyotrophic lateral sclerosis. Muscle Nerve 59, 303–308. https://doi.org/10.1002/mus.26385.
Pan, H., Luo, C., Li, R., Qiao, A., Zhang, L., Mines, M., et al., 2008. Cyclophilin A is required for CXCR4-mediated nuclear export of heterogeneous nuclear ribonucleoprotein A2, activation and nuclear translocation of ERK1/2, and chemotactic cell migration. J. Biol. Chem. 283, 623–637. https://doi.org/10.1074/jbc.M704934200.
Paré, B., Lehmann, M., Beaudin, M., Nordström, U., Saikali, S., Julien, J.-P., et al., 2018. Misfolded SOD1 pathology in sporadic amyotrophic lateral sclerosis. Sci. Rep. 8, 14223. https://doi.org/10.1038/s41598-018-31773-z.
Parker, S.J., Meyerowitz, J., James, J.L., Liddell, J.R., Crouch, P.J., Kanninen, K.M., et al., 2012. Endogenous TDP-43 localized to stress granules can subsequently form protein aggregates. Neurochem. Int. 60, 415–424. https://doi.org/10.1016/j.neuint.2012.01.019.
Pasanen, P., Myllykangas, L., Siitonen, M., Raunio, A., Kaakkola, S., Lyytinen, J., et al., 2014. Novel α-synuclein mutation A53E associated with atypical multiple system atrophy and Parkinson's disease-type pathology. Neurobiol. Aging 35https://doi.org/10.1016/j.neurobiolaging.2014.03.024. (2180.e1-5).
Poesen, K., Van Damme, P., 2018. Diagnostic and prognostic performance of neurofilaments in ALS. Front. Neurol. 9, 1167. https://doi.org/10.3389/fneur.2018.01167.
Seyfried, N.T., Gozal, Y.M., Donovan, L.E., Herskowitz, J.H., Dammer, E.B., Xia, Q., et al., 2012. Quantitative analysis of the detergent-insoluble brain proteome in frontotemporal lobar degeneration using SILAC internal standards. J. Proteome Res. 11,

2721–2738. https://doi.org/10.1021/pr2010814.
Smith, C., Malek, N., Grosset, K., Cullen, B., Gentleman, S., Grosset, D.G., 2019. Neuropathology of dementia in patients with Parkinson's disease: a systematic review of autopsy studies. J. Neurol. Neurosurg. Psychiatry. https://doi.org/10.1136/jnnp-2019-321111.
Steinacker, P., Feneberg, E., Weishaupt, J., Brettschneider, J., Tumani, H., Andersen, P.M., et al., 2016. Neurofilaments in the diagnosis of motoneuron diseases: a prospective study on 455 patients. J. Neurol. Neurosurg. Psychiatry 87, 12–20. https://doi.org/10.1136/jnnp-2015-311387.
Vallarola, A., Sironi, F., Tortarolo, M., Gatto, N., De Gioia, R., Pasetto, L., et al., 2018. RNS60 exerts therapeutic effects in the SOD1 ALS mouse model through protective glia and peripheral nerve rescue. J. Neuroinflammation 15, 65. https://doi.org/10.1186/s12974-018-1101-0.
Verde, F., Silani, V., Otto, M., 2019b. Neurochemical biomarkers in amyotrophic lateral sclerosis. Curr. Opin. Neurol. 32, 747–757. https://doi.org/10.1097/WCO.0000000000000744.
Verde, F., Steinacker, P., Weishaupt, J.H., Kassubek, J., Oeckl, P., Halbgebauer, S., et al., 2019a. Neurofilament light chain in serum for the diagnosis of amyotrophic lateral sclerosis. J. Neurol. Neurosurg. Psychiatry 90, 157–164. https://doi.org/10.1136/jnnp-2018-318704.
Westeneng, H.-J., Debray, T.P.A., Visser, A.E., van Eijk, R.P.A., Rooney, J.P.K., Calvo, A., et al., 2018. Prognosis for patients with amyotrophic lateral sclerosis: development and validation of a personalised prediction model. Lancet Neurol. 17, 423–433. https://doi.org/10.1016/S1474-4422(18)30089-9.
Xiang, S., Kato, M., Wu, L.C., Lin, Y., Ding, M., Zhang, Y., et al., 2015. The LC domain of hnRNPA2 adopts similar conformations in hydrogel polymers, liquid-like droplets, and nuclei. Cell 163, 829–839. https://doi.org/10.1016/j.cell.2015.10.040.
Yang, H.-S., Yu, L., White, C.C., Chibnik, L.B., Chhatwal, J.P., Sperling, R.A., et al., 2018. Evaluation of TDP-43 proteinopathy and hippocampal sclerosis in relation to APOE ε4 haplotype status: a community-based cohort study. Lancet Neurol. 17, 773–781. https://doi.org/10.1016/S1474-4422(18)30251-5.
Yokota, O., Davidson, Y., Bigio, E.H., Ishizu, H., Terada, S., Arai, T., et al., 2010. Phosphorylated TDP-43 pathology and hippocampal sclerosis in progressive supranuclear palsy. Acta Neuropathol. (Berl.) 120, 55–66. https://doi.org/10.1007/s00401-010-0702-1.